Radical stability and its role in synthesis and catalysis

Johnny Hioe and Hendrik Zipse*

Received 16th March 2010, Accepted 18th May 2010
First published as an Advance Article on the web 11th June 2010
DOI: 10.1039/c004166a

The thermodynamic stability of carbon-centered radicals may be defined in quantitative terms using the hydrogen transfer reaction shown in eqn (a). The stability values obtained in this way for substituted systems may be understood as the stabilizing or destabilizing influence of substituents on the neighboring radical center. This approach can be easily adapted to oxygen- or sulfur-centered radicals as expressed in eqn (b).

$$\bullet CH_3 + R{-}H \xrightarrow{\Delta H_{rxn}} CH_4 + R\bullet \quad \text{(a)}$$

$$\bullet XH + RX{-}H \xrightarrow{\Delta H_{rxn}} XH_2 + RX\bullet \quad \text{(b)}$$

The stability values obtained in this way do not only serve as a quantitative basis for the discussion of substituent effects, but also allow for quantitative estimates of reaction energies for hydrogen transfer reactions. These occur as key steps in a multitude of synthetically useful radical-chain processes in apolar solution, in enzyme-mediated non-chain processes in biological systems, and in the oxidative degradation of a variety of biomolecules. The review will highlight the usefulness of radical stability values for the rationalization of successful (and not so successful) synthetic radical reactions as well as the potential design of new radical reactions.

Introduction

The understanding of radical reactions has dramatically profited from decade-long efforts to accurately measure reaction rates for a multitude of processes involving open shell species.[1–4] This is equally true for synthetically important chain reactions in apolar solution as well as for non-chain processes in biological systems in polar media. Based on these data the outcome of reactions involving "typical" species can be predicted with some accuracy. In contrast to many other synthetically useful reaction types, this opens the opportunity to actually design new radical chain reactions in organic synthesis.[5,6] Successful rate measurements can, of course, only be performed for processes with a sufficiently large thermochemical driving force. Theoretically calculated thermochemical data do not suffer from such a selection criterion and are easily available for strongly exothermic and endothermic processes alike. Also, theoretical calculations can be performed with comparable effort on "typical" and "untypical" species, thus facilitating exploratory studies of systems that have not yet been

Department of Chemistry, LMU München, Butenandtstrasse 5-13, D-81377 München, Germany. E-mail: zipse@cup.uni-muenchen.de

Johnny Hioe

Johnny Hioe was born on 16th June 1983 in Jakarta and is a native of Indonesia. He studied chemistry at Ludwig-Maximilians-University of Munich from 2004 to 2009 (M.Sc.). In 2009 he started his Ph.D. studies in the group of Prof. Zipse where he focuses on radical reactions in enzymatic catalysis.

Hendrik Zipse

Hendrik Zipse received his Ph.D. from the University of Basel (Switzerland) in 1991 working in the group of Prof. B. Giese. After a postdoctoral stint with Prof. Ken Houk at UCLA in Los Angeles, he started his independent career at the TU Berlin in 1993 as an assistant professor of organic chemistry. In 1998 he moved to his current position as associate professor of organic chemistry at the LMU Munich. His research interests revolve around the principles of physical organic chemistry and their application to synthetic and catalytic processes.

studied experimentally. It is the purpose of this account to illustrate the usefulness of theoretically calculated radical stability data for analyzing multi-step radical reactions.

Definitions of radical stability

The stability of C-centered radicals can conveniently be expressed using the isodesmic[7] H-transfer reaction shown in eqn (1).[8–10] The reaction enthalpy of this process is commonly referred to as the radical stabilization energy (RSE) of the newly formed radical $^{\bullet}CR_1R_2R_3$ relative to the unsubstituted methyl radical $^{\bullet}CH_3$ (**1**). For isopropyl radical **4**, for example, a RSE value of –26.8 kJ mol^{-1} is derived in this way and interpreted as the result of stabilizing (hyperconjugative) interactions between the two methyl groups and the radical center.[11–13] It should be noted here that this reaction energy is, of course, exactly identical to the difference in the C–H bond dissociation energy in methane (**2**) of BDE(CH_3–H) = +439.3 ± 0.4 kJ mol^{-1}, and that of the central C–H bond in propane (**3**) with BDE$(CH_3)_2$CH–H = +412.5 ± 1.7 kJ mol^{-1}.[11–14]

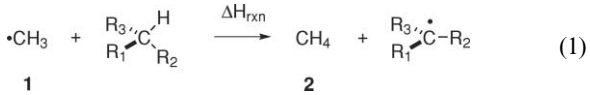

(1)

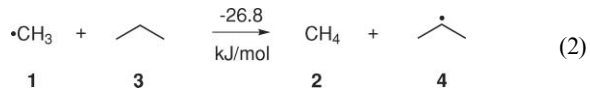

(2)

While it is convenient to interpret the RSE values derived from eqn (1) as the result of stabilizing/destabilizing interactions between the unpaired spin and substituents R_1–R_3, this analysis ignores possible substituent effects in the closed shell reference system $HCR_1R_2R_3$.[9,15] An alternative approach therefore defines radical stabilization energies with reference to a C–C bond cleavage (instead of C–H cleavage) process, as expressed by isodesmic eqn (3). In this particular example methyl radical (**1**) formally abstracts a methyl group from isobutane (**5**), forming isopropyl radical (**4**) and ethane (**6**). Comparison of the defining eqn (2) and (3) shows that only the closed shell reference compounds, not the open shell systems have been modified. The reaction energy for the example in eqn (3) (and thus the RSE of radical **4**) now amounts to –6.5 kJ mol^{-1}, significantly less than that obtained from eqn (2). Thus, while both approaches find the isopropyl radical (**4**) to be more stable than methyl radical (**1**), the actual degree of stabilization differs quite significantly.

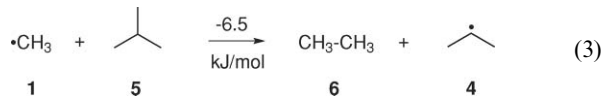

(3)

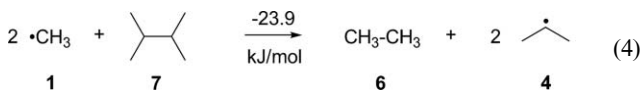

(4)

A third way of quantifying the stability of isopropyl radical (**4**) is based on symmetric reference compound **7**. Cleavage of the fully apolar central C–C bond in **7** (due to symmetry) yields two isopropyl radicals (**4**). Comparison of this cleavage reaction with that of the central C–C bond in ethane (**6**) as expressed in eqn (4) yields a reaction energy of –23.9 kJ mol^{-1}. Due to the fact that eqn (4) involves two methyl radicals (**1**) and two isopropyl radicals (**4**), the corresponding RSE value for radical **4** now equates to –23.9/2 = –11.9 kJ mol^{-1}. This is quite similar to the result obtained from eqn (3), but may also reflect some repulsive interactions between the two isopropyl fragments in the formal dimer **7**. While eqn (3) and (4) are certainly more appropriate for the quantification of substituent effects on radical centers, the approach described by eqn (1) and (2) has the advantage of relating directly to an important elementary process in radical chemistry, the hydrogen transfer reaction between two radicals. These processes are of outstanding importance in synthetic as well as biological radical reactions and often involve hydrogen exchange between carbon- and heteroatom-centered radicals. The stabilities of these latter species can, of course, be defined in a completely analogous way as expressed for carbon-centered radicals in eqn (1), and defining equations for oxygen- and sulfur-centered radicals are given in eqn (5) and (6).

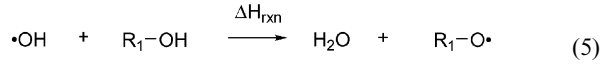

(5)

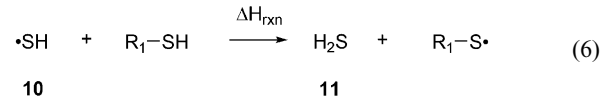

(6)

Together with the experimentally derived bond dissociation energies[14] of the reference systems CH_4 (BDE(CH_3–H) = +439.3 kJ mol^{-1}), H_2O (BDE(HO–H) = +497.1 kJ mol^{-1}) and H_2S (BDE(HS–H) = +381.2 kJ mol^{-1}), this provides a basis for the comparative description of the stability of carbon- and heteroatom-centered radicals as shown in Fig. 1. The corresponding RSE and BDE data have been collected in Table 1.

The RSE values shown for carbon-centered radicals in Fig. 1 have been selected to reconfirm the textbook-level view of radical stability: primary radicals such as ethyl radical (**12**) are less stable than secondary radicals such as isopropyl radical (**4**), and those are less stable than tertiary radicals such as *t*-butyl radical (**13**). The stabilizing effects of resonance interactions, as present in allyl radical (**14**), far exceed those of simple alkyl groups and lead to exceedingly stable spin-delocalized systems. Phenyl radical **15**, in contrast, is significantly less stable than other alkyl radicals due to the much higher bond strength of aromatic C–H bonds. What is generally less well known (simply due to the lack of appropriate data) is how these stability values relate to those of heteroatom centered radicals. From Fig. 1 it is, for example, quite obvious that the stability of glycyl peptide radical **16** is quite comparable to that of cysteinyl radical **17** and phenoxy radicals **18** and **19** (acting as mimics of tyrosyl radicals). The high (and comparable) stability of these protein-derived radicals, whose role in enzymatic catalysis is undisputed, contrasts remarkably with that of cofactor-derived 5′-desoxy-5′-adenosyl radical (**59**). The stability of this latter species is quite comparable to that of other primary radicals and the control of this thermochemically "hot" species may thus require considerably more effort from the side of the enzyme than that of the much more stable protein-bound species **16–19**. Also apparent from Fig. 1 is the much larger range of RSE values for O-centered radicals than for C-centered or for S-centered radicals. The RSE difference between alkoxy radical **20** and phenoxy radical **18**, for example, is significantly larger at 74 kJ mol^{-1} than the difference between alkylthiyl radical **44** and thiophenyl radical **21**

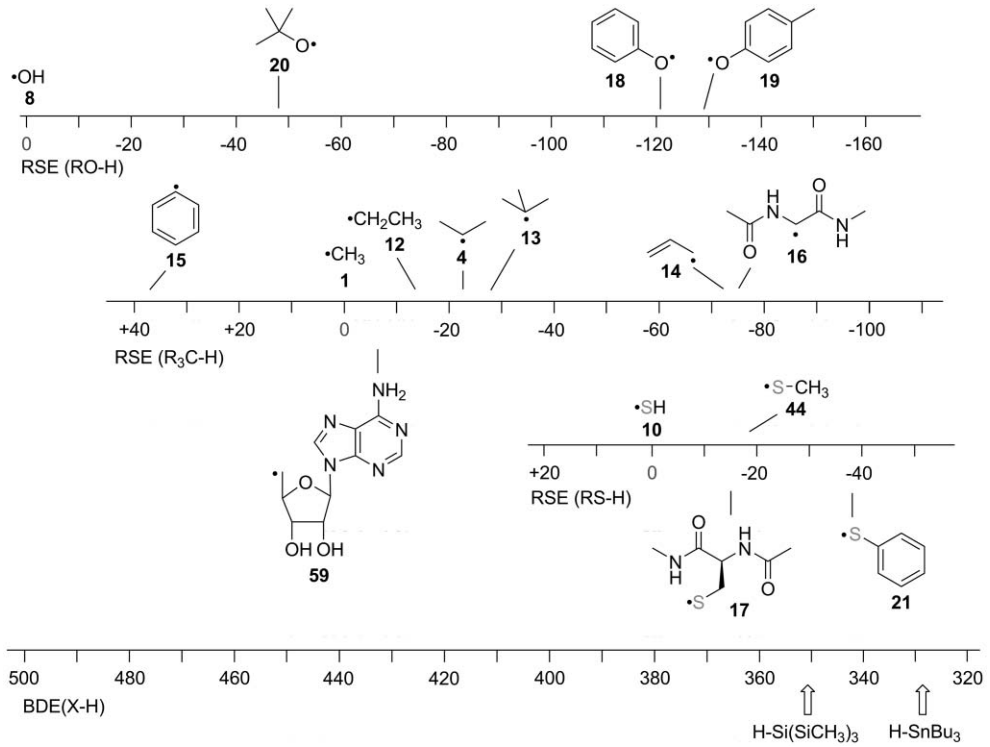

Fig. 1 RSE data for selected O-, C-, and S-centered radicals together with BDE data for hydrogen donors $HSi(SiMe_3)_3$ and $HSnBu_3$.

of 20 kJ mol^{-1}. This reflects to a large degree the electron deficient nature of O-centered radicals and the correspondingly large effects of electron-donating alky and aryl substituents.

In the following we will use the RSE values in Table 1 to illustrate the use of this type of thermochemical data in rationalizing the design of successful synthetic radical reactions as well as non-chain processes in biological systems.

Protecting group/radical translocation (PRT) reactions

A first application of the RSE/BDE data shown in Fig. 1 concerns the rationalization of complex sequences of radical reactions involving hydrogen transfer steps as key elements. One such scheme, termed "protecting/radical translocating (PRT)" reactions, involves the use of protecting groups with the added function of translocating an initially formed radical to the actual substrate of the reaction.[16,17] The example selected for this class of reactions involves the *o*-iodobenzyl protecting group for alcohols.[17a] Under standard tin hydride conditions the protecting group can be activated through iodine atom abstraction by tin radicals (Scheme 1). Aryl radical **23** generated in this step can then undergo 1,5-hydrogen migration yielding alkyl radical **24**, or react with $HSnBu_3$ in a bimolecular fashion to yield the acyclic product **25**. Radical **24** is ideally poised to undergo 5-*exo*-trig cyclization with the acrylate double bond yielding cyclic radical **26**, whose trapping by $HSnBu_3$ yields the cyclic product **27** as a 1 : 4 mixture of *cis*/*trans* isomers. The ratio of acyclic and cyclic products will undoubtedly depend on the tin hydride concentration and a ratio of 37 : 63 has been reported in the literature.[17a] RSE and BDE values can be used to verify the thermochemical feasibility of three of the five steps shown in Scheme 1 by selecting stability data of structurally similar radicals. The stability of radical **23**, for example, can be quantified with that of the phenyl radical (**15**), while that of the subsequently formed alkyl radical **24** can be approximated with 2-methoxyprop-2-yl radical **28**. The RSE value of this latter radical amounts to −36.3 kJ mol^{-1} (relative to methyl radical **1**), while the phenyl radical is significantly less stable at RSE(**15**) = +37.0 kJ mol^{-1}. With these values in hand we can estimate the intramolecular 1,5-hydrogen transfer step to be exothermic by 73.3 kJ mol^{-1}. Theoretically calculated RSE values can be combined with experimental data for Sn–H bond cleavage in $HSnBu_3$ with BDE(Sn–H) = 328.9 kJ mol^{-1}[18,19] to assess the thermochemical feasibility of the two intermolecular hydrogen transfer steps shown in Scheme 1. The first of these converts radical **23** to closed shell product **25** and tin radical $^{\bullet}SnBu_3$. Assuming again that the stability of radical **23** can be quantified by that of phenyl radical (**15**), this step is predicted to be strongly exothermic by 147 kJ mol^{-1}. The second hydrogen transfer step involving $HSnBu_3$ converts cyclic radical **26** to closed shell product **27**. Assuming that the stability of **26** can be modeled satisfactorily by that of $^{\bullet}CH(CH_3)(CO_2Et)$ (**29**) with RSE = −42.0 kJ mol^{-1}, this hydrogen transfer step is predicted to be exothermic by 68.4 kJ mol^{-1}. In summary, the RSE/BDE analysis shows that all hydrogen transfers steps in Scheme 1 are perfectly reasonable from a thermochemical perspective.

The graphical display of the RSE and BDE data cited above in Fig. 2 also indicates that trapping of radical **24** (whose stability is comparable to that of **28**) by $HSnBu_3$ is also quite exothermic (by 74.1 kJ mol^{-1}). This implies that acyclic product **25** can, in principle, also be formed by the trapping of radical **24**. Stability data available in the literature for a variety of radicals also suggest

Table 1 Radical stabilization energies (RSE, in kJ mol^{-1}) at 298.15 K of the systems shown in Fig. 1 and X–H bond dissociation energies of the respective closed shell compounds

System	G3(MP2)-RAD	Other	RSE exp.[a]	BDE(X-H) exp.[a]
$^{\bullet}C_6H_5$ (**15**)	+37.0[b]	+48.4 (G3B3)[b]	+32.9	+472.2 ± 2.2
$^{\bullet}CH_3$ (**1**)	0.0	0.0	0.0	+439.3 ± 0.4
5′-Desoxy-5′adenosyl (**59**)	−6.8[c]			
$^{\bullet}CH_2CH_3$ (**12**)	−13.5[b]	−13.8 (G3B3)[b]	−18.8	+420.5 ± 1.3
		−15.1 (W1)[b]		
$^{\bullet}CH_2OC(O)CH_3$ (**55**)	−18.4[b]	−17.9 (W1)[b]	−34.7	+404.6
$^{\bullet}CH(CH_3)CH_2CH_3$ (**45**)	−19.5[b]	−21.2 (G3)[f]	−28.0	+411.1 ± 2.2
$^{\bullet}CH(CH_3)_2$ (**4**)	−23.0[b]	−22.2 (G3)[f]	−26.8	+412.5 ± 1.7
$^{\bullet}CH_2C(O)N(H)CH_3$ (**53**)	−23.0[b]			
$^{\bullet}CH_2C(O)OCH_3$ (**56**)	−23.0[b]	−25.0 (W1)[b]	−30.0	+406.3 ± 10.5
$^{\bullet}C(CH_3)_3$ (**13**)	−28.5[b]	−28.4 (G3)[f]	−38.9	+400.4 ± 2.9
$^{\bullet}C(OCH_3)(CH_3)_2$ (**28**)	−36.3[b]			
$^{\bullet}CH(OCH_3)(CH_3)$ (**30**)	−36.5[b]			
$^{\bullet}CH(CH_3)(CON(CH_3)_2)$ (**31**)	−38.6[b]			
$^{\bullet}CH(CH_3)(COOEt)$ (**29**)	−42.0[b]			
$^{\bullet}C(CH_3)_2OH$ (**57**)	−41.1[b]	−40.8 (G3)[f]	−42.8	+396.5
$^{\bullet}CH_2NHC(O)CH_3$ (**54**)	−43.0[b]			
$^{\bullet}CH(CH_3)(NHCOCH_3)$ (**32**)	−45.7[b]			
$^{\bullet}CH(CH_3)COCH_3$ (**58**)	−53.9[b]	−52.2 (G3)[f]	−53.1	+386.2 ± 7.1
$^{\bullet}CH(CH_3)(N(CH_3)_2)$ (**33**)	−54.6[b]			
$^{\bullet}CH(CH_3)(C_6H_5)$ (**34**)	−68.3[b]		−81.7	+357.6 ± 6.3
$^{\bullet}CHCHCH_2$ (**14**)	−72.0[b]	−70.5 (G3B3)[b]	−70.7	+368.6 ± 2.9
		−71.6 (W1)[b]		
$CH_3CONHCH^{\bullet}CONHCH_3$ (**16**)	−74.1[c]	−75.5 (G3B3)[c]		
Cyclohexa-1,4-dien-3-yl (**47**)		−119.5 (G3)[f]	−121.3	+318.0 ± 5.0
			−117.6[h]	+321.7 ± 2.9[g]
$^{\bullet}OH$ (**8**)	0.0	0.0	0.0	+497.1 ± 0.3
$^{\bullet}OC(CH_3)_3$ (**20**)	−47.5	−47.7 (G3B3)	−52.2	+444.9 ± 2.8
$^{\bullet}OC_6H_5$ (**18**)	—	−121.6 (G3B3)[c]	−134.3	+362.8 ± 2.9
			−132.6[c]	
$^{\bullet}OC_6H_5CH_3$ (**19**)	—	−129.4 (G3B3)[c]	−136.9	+360.2 ± 2.1
			−140.7[c]	
$^{\bullet}SH$ (**10**)	0.0	0.0	0.0	+381.2 ± 0.1
				+376.2 ± 0.1 (0 K)[d]
$^{\bullet}SCH_3$ (**44**)	−18.1[c]	−18.2 (G3B3)[c]	−15.5	+365.7 ± 2.1
$^{\bullet}$S–Cys (**17**)	−13.7[c]	−14.4 (G3B3)[c]		
$^{\bullet}SC_6H_5$ (**21**)	−43.6	−38.2 (G3B3)	−31.8	+349.4 ± 4.5
			−40.9 (0 K)[e]	
			−40.8 (298 K)[e]	+335.3 ± 1.2 (0 K)[e]

[a] All BDE data at 298.15 K taken from ref. 14, if not specified otherwise. [b] Taken from ref. 9; [c] Taken from ref. 10. [d] Taken from ref. 24. [e] Obtained from the value at 0 K in combination with the G3B3 thermal corrections. [f] Taken from ref. 34. [g] Taken from ref. 25.

that many alternative linker structures between protecting group and substrate are compatible with the requirement of exothermic 1,5-H transfer.

The stability of tertiary radical **28**, for example, is practically identical to that of secondary radical **30**. This implies that secondary alcohols will show similar PRT reactions to tertiary alcohols of analogous structure, well in line with available experimental data.[17a] The use of carboxylate linkers (leading to radicals such as **31**) and amide or amine linkers (leading to radicals such as **32** and **33**) have been suggested in the literature[17c] and the RSE analysis again reveals that all of these functionalities will provide similarly exothermic 1,5-H transfer reactions. The use of simple hydrocarbon functionalities is usually not well compatible with protecting group concepts due to problems in installation and removal, but the stability data for benzyl radical **34** and secondary radical **4** show that even simple alkyl chains will act as hydrogen donors for 1,5-H shift reactions with aryl radicals in an exothermic fashion. This is again well in line with available experimental data.[17c]

Polarity reversal catalysis (PRC)

Homolytic hydrogen transfer reactions can be accelerated considerably by tuning the polarity of the hydrogen atom donors and acceptors in an appropriate fashion. It is, for example, well known that electrophilic alkoxy radicals will abstract hydrogen from electron-rich C–H bonds faster than from electron-deficient substrates with comparable C–H bond energies. This insight has been developed into a general design concept for radical chain reactions commonly referred to as "polarity reversal catalysis (PRC)".[20] While it is important to acknowledge that PRC builds on the concept of barrier reduction through lowering the intrinsic barriers for hydrogen transfer reactions, thermochemical criteria such as RSE data for the participating open shell species are nevertheless useful in defining the limits of this type of catalysis. A recent example for PRC catalysis involving combinations of different H-atom donors is shown in Scheme 2.[21,22]

This involves the reaction of cyclohexadiene **36** acting not only as an organic H-atom donor, but also as a source of

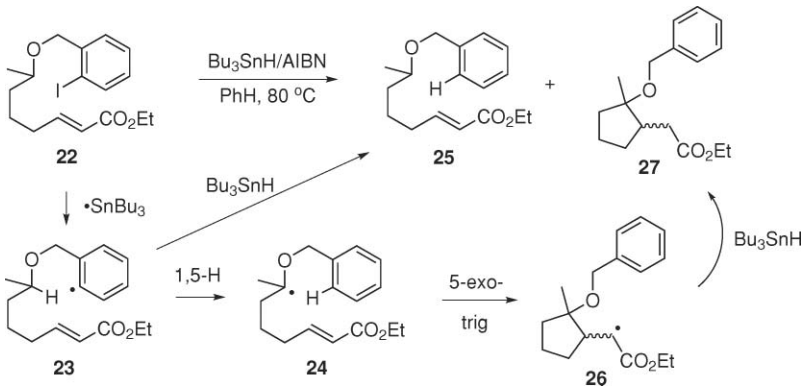

Scheme 1 Example for protecting group/radical translocation (PRT) reaction.[17a]

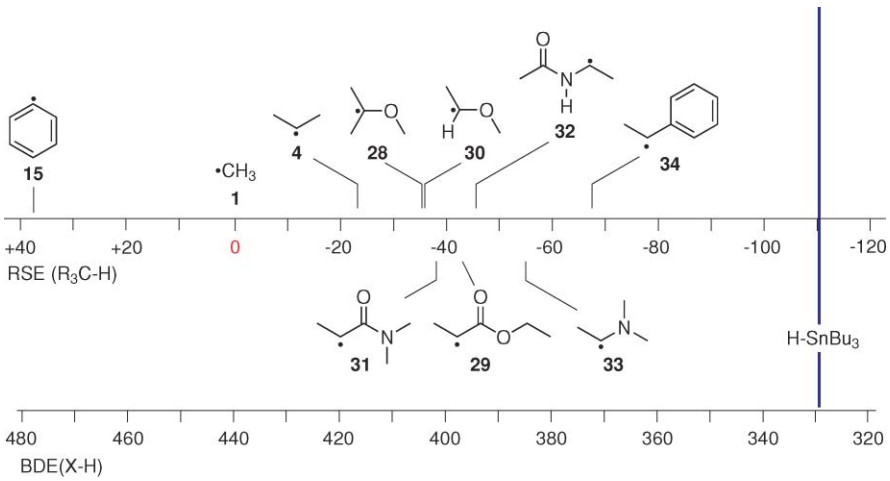

Fig. 2 RSE data for radicals related to the reaction mechanism shown in Scheme 1 together with BDE data for H-$SnBu_3$.

aminyl radicals. Both functions taken together allow for the hydroamination of unfunctionalized alkenes such as 1-octene (**35**), in this case yielding 50% of a 7 : 1 mixture of regioisomeric amides **37** and **38**. The reaction is initiated by 0.5 equiv. of di-*t*-butylperoxide (DTBP) in benzene solution, but proceeds significantly better in the presence of 0.2 equiv. thiophenol (HSPh, **39**). A reaction mechanism accounting for this finding is shown in Scheme 3. Initial H-atom abstraction from cyclohexadiene **36** through peroxy radicals generated from DTBP yields radical **40** as one of the chain-carrying radicals in this system. Cyclohexadienyl radical **40** will eliminate aminyl radical **41** together with benzene derivative **42** through unimolecular C–N bond cleavage. Addition of aminyl radical **41** to 1-octene (**35**) can, in principle, proceed in anti-Markovnikov fashion to yield adduct radical **43** or in Markovnikov fashion yielding the regioisomeric adduct radical (not shown).

Adduct radical **43** is converted to closed-shell product **37** through (fast) H-atom abstraction from thiophenol **39**, yielding thiyl radical **21** as the fourth chain-carrying radical in this system. Reaction of **21** with cyclohexadiene **36** then closes the catalytic cycle and regenerates the catalytic thiol **39**. The catalytic function of thiol **39** thus boils down to replacing one hydrogen transfer reaction between two carbon centers by two separate H-atom transfer steps between carbon and sulfur. The criteria for this type of catalysis can readily be visualized using radical stability scales for C- and S-centered radicals (Fig. 3). The H–S BDE in thiophenol (**39**) has recently been redetermined by Ashfold *et al.* through gas phase measurements at 0 K and a value of BDE(S–H, **39**, 0 K) = 335.3 ± 1.2 kJ mol^{-1} has been derived.[23] Combination of this value with that for the reference system H_2S (**10**) of BDE(S–H, **10**, 0 K) = 376.2 ± 0.1 kJ mol^{-1}[24] yields RSE(**21**) = –40.9 kJ mol^{-1} at 0 K.[10] Using the (rather small) thermochemical corrections to 298.15 K used in the G3B3 scheme one can also predict a value of RSE(**21**) = –40.8 kJ mol^{-1} at 298.15 K. This implies that radical **21** is significantly more stable than aliphatic thiyl radicals such as methylthiyl radical (**44**) or cysteinyl radical **17**. Turning to the catalytic cycle shown in Scheme 3, the stability of radical **21** is relevant in two of the four steps. In the first of these, thiophenol (**39**) reacts with secondary radical **43**, whose stability may be assumed to be similar to that of isopropyl radical (**4**) or but-2-yl radical (**45**). Adopting the RSE data available for the latter of these systems at the G3 level of RSE(**45**) = –21.2 kJ mol^{-1} implies a (highly favorable!) reaction energy of –77.7 kJ mol^{-1} for the hydrogen transfer between radical **43** and thiophenol (**39**). The properties of cyclohexadiene **36** can be approximated with those of the parent cyclohexa-1,4-diene (**46**). The stability of the corresponding radical **47** of RSE(**47**) = –119.5 kJ mol^{-1} at the G3 level is quite close to previous[14] and more recent experimental and high-level theoretical studies.[25] Assuming this value also to be valid for the more highly substituted cyclohexadiene radical **40** in

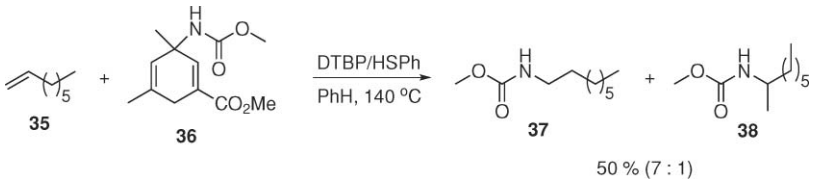

Scheme 2 Polarity reversal catalysis (PRC) as applied to the hydroamination of 1-octene (**35**).[22]

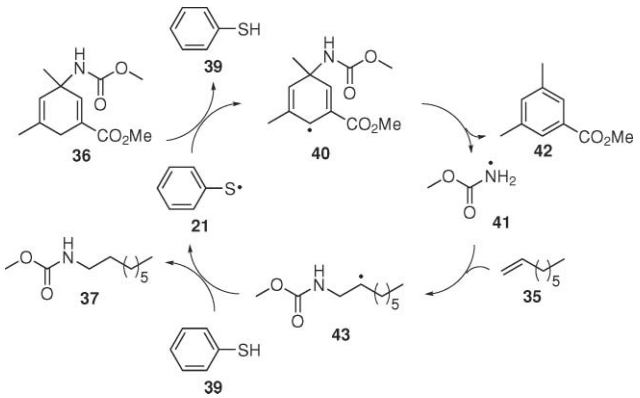

Scheme 3 Radical chain reaction for the PRC example shown in Scheme 2.[22]

Scheme 3 implies that the reaction of thiophenyl radical **21** with cyclohexadiene **36** is indeed exothermic by 20.6 kJ mol^{-1}. The art in designing and optimizing PRC reactions is thus connected to finding a thiol whose BDE(S–H) is located in-between that of the breaking C–H bond and that of the new C–H bond being made.

Biomimetic oxidation reactions

Oxidation reactions of small peptide systems have been studied widely as models for oxidative stress of proteins.[26,27] The example shown in Scheme 4 involves the treatment of glycyl peptide **48** with di-*t*-butyl peroxide (DTBP, **49**) in apolar solution.[28] This reaction yields dimer **50** in 51% yield, a result readily rationalized by the sequence shown in Scheme 4: (a) initial homolysis of the O–O bond in peroxide **49** yields two *t*-butoxy radicals **20**; (b) hydrogen abstraction by radical **20** from the C_α position of peptide **48** generates peptide radical **51** and *t*-butanol **52**; (c) dimerization of peptide radical **51** yields dimer **50**. The formation of dimer **50** in fair yield is hardly compatible with the "flame thrower" picture of alkoxy radicals as highly reactive and unselective species in hydrogen abstraction reactions. Instead, it appears that either kinetic or thermodynamic control mechanisms exist leading to highly selective hydrogen abstraction from the C_α position of glycyl peptide **48**.

The thermodynamics of all possible C–H abstraction reactions in this system can be assessed in a straightforward way by comparing the stabilities of C-centered radicals of appropriate structure. Data for glycyl radical **51** appear not to be available, but the stability of related radical **16** has been characterized in several studies.[10,29] The high value of RSE(**16**) = −75.5 kJ mol^{-1} at the G3B3 level is the result of the simultaneous presence of donor substituents (as in acetamide radical **53** with RSE(**53**) = −23.0 kJ mol^{-1}) and acceptor substituents (as in acetamide radical **54** with RSE(**54**) = −43.0 kJ mol^{-1}) at the same radical center.[8,10,29,30] This implies an extra stabilization of 9.5 kJ mol^{-1} through "captodative" stabilization effects. The ester terminus in substrate **48** can, of course, also act as H atom donor. The stability of the resulting radical can best be modeled with that of methyl acetate radical **55**, whose stability is significantly lower than that of any other system discussed so far at RSE(**55**) = 17.9 kJ mol^{-1}. The main structural difference between glycyl peptide radicals **51** and **16** exists on the C-terminal side, where a methyl ester is present in **51** and a methyl amide in **16**. The stabilizing effects of these two fragments on adjacent radical centers is, however, quite

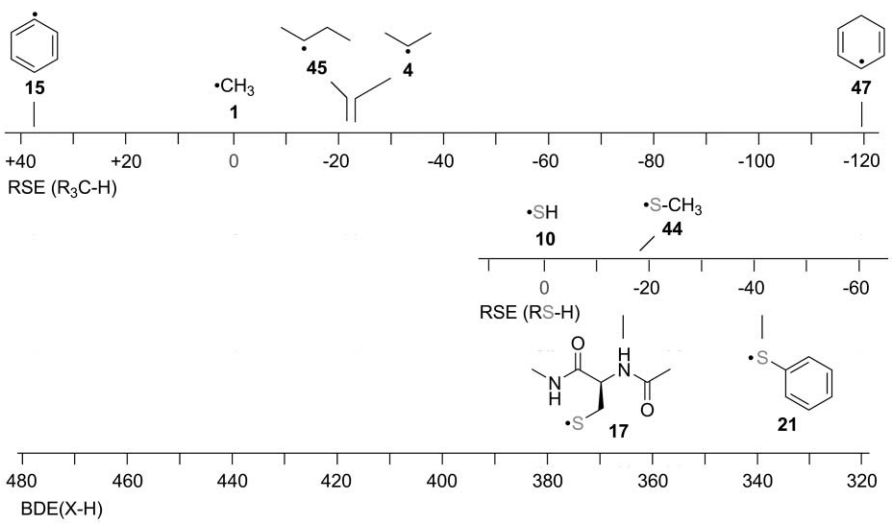

Fig. 3 RSE data for radicals related to the reaction mechanism shown in Scheme 3.

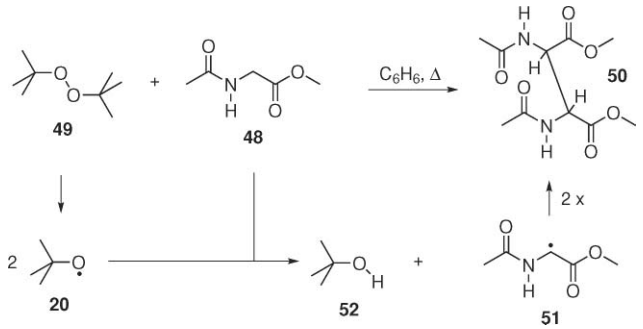

Scheme 4 Oxidative "stress test" for glycyl peptide **48**.[28]

comparable, as can be seen from the stabilities of methyl acetate radical **56** with RSE(**56**) = –25.0 kJ mol^{-1}) and methyl acetamide radical **53** with RSE(**53**) = –23.0 kJ mol^{-1}. We may thus conclude that radical **16** can serve as a sufficiently accurate model of **51**.

Finally, H abstraction in glycine derivative **48** can also occur from the amide N–H fragment. We exclude this possibility here because previous theoretical studies (performed at CBS-QB3 level at 0 K) indicate that homolytic N–H bond cleavage is more than 100 kJ mol^{-1} less favorable than C_α–H cleavage in dipeptide models.[32] Alkoxy radicals such as the *t*-butoxy radical (**20**) with RSE(**20**) = –47.7 kJ mol^{-1} are significantly more stable than the parent hydroxy radical HO$^\bullet$ (**8**), but much less stable than the phenoxy radicals **18** and **19**. Graphical display of the respective RSE values in Fig. 4 shows that practically all possible C–H abstraction reactions involving glycine peptide model **48** and *t*-butoxy radical **20** are exothermic. The degree of exothermicity is largest for hydrogen abstraction from the C_α position with a reaction energy of –85.5 kJ mol^{-1}. The experimentally found preferred formation of dimer **50** can thus be rationalized by assuming that, at least under the selected reaction conditions, only the thermochemically most stable radicals are formed. *t*-Butoxy radical **20** would then be highly selective in its choice of the reaction site. Alternatively, it may be assumed that radical **20** generates a variety of C-centered radicals in a primary (unselective) hydrogen abstraction step, but that subsequent equilibration among these C-centered radicals reduces the population of the less stable species, eventually leaving **51** as the most stable radical behind. In either case we can clearly see from Fig. 4 that the experimental reaction outcome can easily be rationalized by assuming thermochemical control of radical formation at some stage. It should be added that a change away from apolar organic solvents towards the biologically more relevant aqueous phase might significantly alter the outcome of this type of experiment.[35]

Radicals in enzymatic catalysis: class I ribonucleotide reductase (RNR I)

Studies on radical enzymes such as class I ribonucleotide reductase (RNR I) or pyruvate formate lyase (PFL), to name two of the best characterized systems, have benefited greatly from recent advances in structural biology, time-resolved spectroscopic techniques and computational chemistry.[36] In particular, the combination of time-resolved EPR spectroscopy with theoretically computed spectral parameters has been highly successful in identifying previously unknown transient species, whose involvement in the substrate mechanism has been discussed long before actual data were available.[37,38] In the following we will show that the soundness of mechanistic proposals can also be tested by estimating the thermodynamic stability of the open shell species involved. This is, of course, particularly relevant in reactions involving hydrogen transfer steps, as RSE differences then translate directly into reaction energies. The example chosen here is that of the substrate mechanism of *e. coli* RNR I as shown in Scheme 5.

After binding of the diphosphate ribonucleotide substrate in the active site of the R1 subunit and generation of a protein-bound thiyl radical at cysteine residue C439 (**A**), the substrate mechanism is initiated by hydrogen abstraction from the C3′ position (**B**). Base-induced elimination of water at the radical stage then yields a new substrate radical (**C**), able to abstract a hydrogen atom from one of the cysteine residues C462 and C225 in the active site (**D**). It is at this stage that the actual reduction

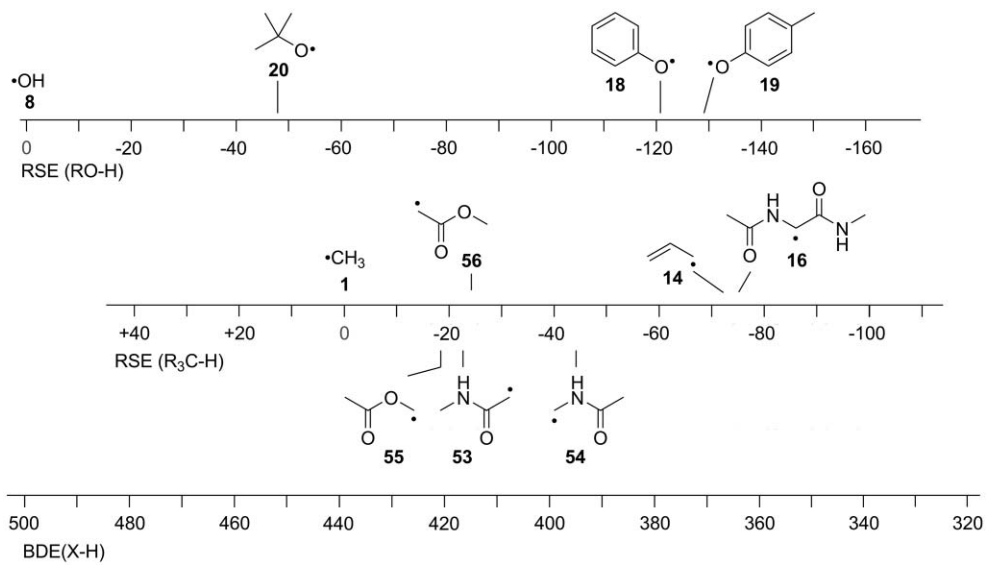

Fig. 4 RSE data for radicals related to the oxidation reaction in Scheme 4.

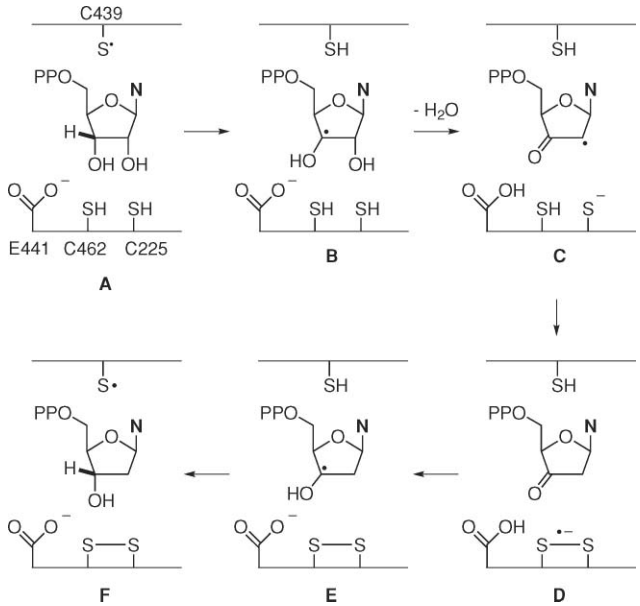

Scheme 5 Substrate reaction mechanism of RNR I from *e. coli*.[36b]

step occurs through (concerted) electron transfer to the C–O double bond at the C3′ position, closely coupled to protonation of the resulting ketyl radical anion by the adjacent glutamic acid residue E441 (**E**). Finally, reabstraction of the hydrogen lost in the first step completes the overall sequence and furnishes the reduced desoxyribonucleotide as the product. Three of the five reaction steps shown in Scheme 5 (**A**/**B**, **C**/**D**, and **E**/**F**) involve hydrogen atom transfer and we can use RSE values of closely related fragment radicals to estimate the thermodynamics of these transformations (Fig. 5). The cysteinyl radical at stage **A** of the substrate mechanism can satisfactorily be modeled with cysteine dipeptide radical **17**, while the substrate radical generated after hydrogen transfer may be most simply represented by isopropanol-2-yl radical **57**.

Positioning these two species on the combined RSE scales as shown in Fig. 5 indicates that the first step of the substrate mechanism will be endothermic by 31.7 kJ mol^{-1}, an unlikely large endothermicity for the first step of a sequence known to work very efficiently under experimental conditions. A number of recent studies using significantly larger model systems, but somewhat inferior theoretical methods, indicate that hydrogen bonding between the C3′ hydroxy group and the glutamate E441 carboxylate group reduces the endothermicity of the hydrogen abstraction by 13–18 kJ mol^{-1}.[39–42] The existence of this type of anionic hydrogen bond deposits somewhat more negative charge on the hydroxy oxygen atom than would normally be the case, which in turn leads to stabilization of the C3′ radical after hydrogen transfer has occurred. This stabilizing effect also implies that the bound substrate at stage **A** of the mechanism in Scheme 5 should be drawn with a strong hydrogen bond between the E441 carboxylate group and the C3′ hydroxy group, as only this situation is in line with the observed reactivity. The second hydrogen transfer step in Scheme 5 transforms the secondary substrate radical at stage **C** into a closed shell intermediate and cysteinyl radical C225/C462. The corresponding radical models chosen here are those of 2-butanone-3-yl radical **58** and again cysteine dipeptide radical **17**. The alignment of these two species in Fig. 5 indicates an exothermicity of the hydrogen transfer step of 20.3 kJ mol^{-1}. Additional interactions of the cysteinyl radical with its anionic neighbor will further enhance this exothermicity. The third (and final) hydrogen transfer step in Scheme 5 transforms the reduced substrate radical of stage **E** to the reduced product and regenerates the initial cysteinyl radical at C439. This mirrors the reverse reaction of the initial substrate activation step, with the difference of the missing hydroxy substituent at the C2′ position of the nucleotide substrate. Theoretical studies on extended substrate systems (using moderately accurate theory) indicate that the presence of this latter substituent is of minor relevance for the H-transfer energetics.[39–42] This implies that the final hydrogen transfer step is as much exothermic as the initial hydrogen transfer step is endothermic. In summary, this analysis shows that, from the three hydrogen transfer steps presented in Scheme 5, only the first faces a thermodynamic hurdle of approx. 14 kJ mol^{-1}. The latter two steps are exothermic and will thus proceed without any thermodynamic penalty.

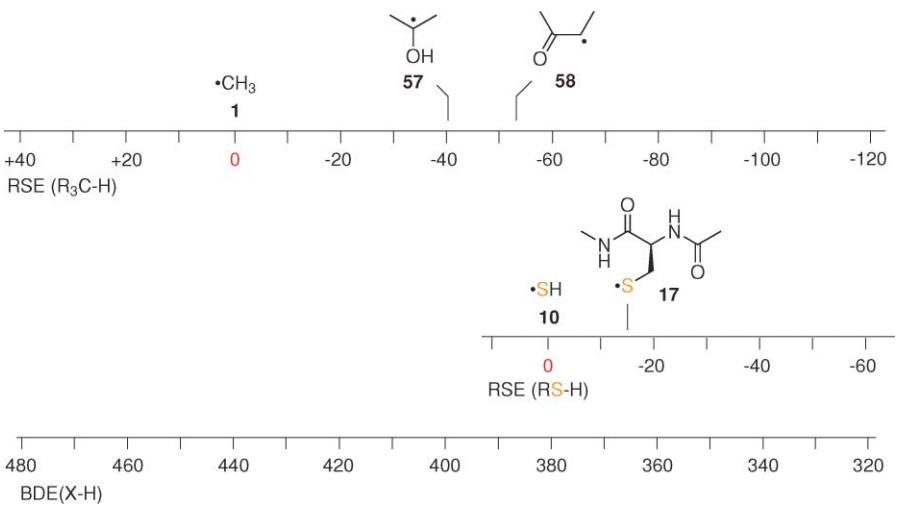

Fig. 5 RSE data for radicals related to the RNR I substrate reaction in Scheme 5.

Conclusions

The moderate charm of thermochemical data such as the RSE values compiled in Table 1 can be enhanced considerably by plotting the respective open shell systems in a graphical manner on a scale relative to the selected reference system, and by combining the scales for C-, S-, and O-centered radicals such that the offset of these scales reflects the differences in experimentally measured BDE values of H–X bonds in the reference systems. In this type of presentation the direct correspondence of RSE and BDE values becomes immediately visible, and exothermic and endothermic radical transformations involving hydrogen transfer reactions are easily recognized in a quantitative manner. Due to the availability of reliable stability values for a large variety of radicals it is not only possible to assess the validity of radical reactions involving hydrogen transfer steps in a quantitative manner, but it is also quite easily possible to identify alternatives of existing methods. A particular strength of the RSE data used here is the ability to predict reaction energies for exo- and endothermic reactions alike, thus providing a valuable addition to kinetic data available in the literature mainly for exothermic reaction steps. The ability to calculate thermodynamic data with acceptable accuracy even for larger model systems also opens the possibility to optimize the properties of new reagents or reactants in a systematic manner. An example for this latter approach is the current design of boron-based reducing reagents.[31–33]

Acknowledgements

We thank the Deutsche Forschungsgemeinschaft (DFG) for funding part of the research presented here through research grant ZI 436/13-1 and the SFB 749 (Dynamics and Intermediates of Molecular Transformations).

References

1 *Landolt-Börnstein: Radical Reaction Rates in Liquids*, Vol. II/18 Springer.
2 H. Fischer and L. Radom, *Angew. Chem., Int. Ed.*, 2001, **40**, 1340–1371.
3 M. Newcomb, *Tetrahedron*, 1993, **49**, 1151–1176.
4 D. Griller and K. Ingold, *Acc. Chem. Res.*, 1980, **13**, 317–323.
5 B. Giese, *Radicals in organic synthesis: formation of carbon-carbon bonds*, Pergamon Press, Oxford, 1986.
6 *Radicals in Organic Synthesis*, ed. P. Renaud and M. P. Sibi, Vol. 1 & 2, John Wiley & Sons, 2001.
7 (*a*) W. J. Hehre, R. Ditchfield, L. Radom and J. A. Pople, *J. Am. Chem. Soc.*, 1970, **92**, 4796; (*b*) S. E. Wheeler, K. N. Houk, P. v. R. Schleyer and W. D. Allen, *J. Am. Chem. Soc.*, 2009, **131**, 2547–2560.
8 H. Zipse, *Top. Curr. Chem.*, 2006, **263**, 163–189.
9 M. Coote, C. Y. Lin, H. Zipse, Carbon Centered Radicals: Structure, Reactivity and Dynamics, in *Reactive Intermediates in Chemistry and Biology*, ed. M. Forbes, Vol. 4 , Wiley, 2010, p. 83–104.
10 J. Hioe and H. Zipse, *Faraday Discuss.*, 2010, **145**, 301–313 and subsequent discussion, p. 381–409.
11 S. J. Blanksby and G. B. Ellison, *Acc. Chem. Res.*, 2003, **36**, 255–263.
12 M. W. Chase, Jr., NIST-JANAF Themochemical Tables, 4th edn, *J. Phys. Chem. Ref. Data, Monograph*, 19989, 1–1951.
13 The following experimental heats of formation and BDE data from references ref. 11 and 14 have been used for the calculation of these RSE values: $\Delta H_{f,298}$(**1**) = +146.7 kJ mol^{-1}; $\Delta H_{f,298}$(**2**) = −74.9 kJ mol^{-1}; $\Delta H_{f,298}$(**4**) = +90.0 kJ mol^{-1}; $\Delta H_{f,298}$(**3**) = −104.7 kJ mol^{-1}; $\Delta H_{f,298}$(**5**) = −134.2 kJ mol^{-1}; $\Delta H_{f,298}$(**6**) = −84.0 kJ mol^{-1}; BDE(C–C,**6**) = 377.4 ± 0.8 kJ mol^{-1}; BDE(C–C,**7**) = 353.5 ± 4.6 kJ mol^{-1}.
14 Y.-R. Luo, *Comprehensive Handbook of Chemical Bond Energies*, CRC Press, 2007.
15 (*a*) A. A. Zavitsas, *J. Chem. Educ.*, 2001, **78**, 417–419; (*b*) N. Matsunaga, D. W. Rogers and A. A. Zavitsas, *J. Org. Chem.*, 2003, **68**, 3158–3172; (*c*) A. A. Zavitsas, *J. Org. Chem.*, 2008, **73**, 9022–9026.
16 A. J. McCarroll and J. C. Walton, *Angew. Chem., Int. Ed.*, 2001, **40**, 2224–2248.
17 (*a*) D. P. Curran, D. Kim, H. T. Liu and W. Shen, *J. Am. Chem. Soc.*, 1988, **110**, 5900–5902; (*b*) D. P. Curran and W. Shen, *J. Am. Chem. Soc.*, 1993, **115**, 6051–6059; (*c*) D. P. Curran and J. Xu, *J. Am. Chem. Soc.*, 1996, **118**, 3142–3147.
18 C. Chatgilialoglu, M. Newcomb, in *Advances In Organometallic Chemistry*, ed. R. West, A. F. Hill, Academic Press, San Diego, 1999, 44, 67–112.
19 L. J. J. Laarhoven, P. Mulder and D. D. M. Wayner, *Acc. Chem. Res.*, 1999, **32**, 342–349.
20 B. P. Roberts, *Chem. Soc. Rev.*, 1999, **28**, 25–35.
21 A. F. Bella, L. V. Jackson and J. C. Walton, *Org. Biomol. Chem.*, 2004, **2**, 421–428.
22 J. Guin, C. Mück-Lichtenfeld, S. Grimme and A. Studer, *J. Am. Chem. Soc.*, 2007, **129**, 4498–4503.
23 A. L. Devine, M. G. D. Nix, R. N. Dixon and M. N. R. Ashfold, *J. Phys. Chem. A*, 2008, **112**, 9563–9574.
24 R. C. Shiell, X. K. Hu, Q. J. Hu and J. W. Hepburn, *J. Phys. Chem. A*, 2000, **104**, 4339–4342.
25 Y. Gao, N. J. DeYonker, E. C. Garrett III, A. K. Wilson, T. R. Cundari and P. Marshall, *J. Phys. Chem. A*, 2009, **113**, 6955–6963.
26 C. J. Easton, *Chem. Rev.*, 1997, **97**, 53–82.
27 M. J. Davies, R. T. Dean, *Radical-Mediated Protein Oxidation: From Chemistry to Medicine*, Oxford University Press, Oxford, 1997.
28 N. Obata and K. Niimura, *J. Chem. Soc., Chem. Commun.*, 1977, 238.
29 G. P. F. Wood, D. Moran, R. Jacob and L. Radom, *J. Phys. Chem. A*, 2005, **109**, 6318–6325.
30 A. K. Croft, C. J. Easton and L. Radom, *J. Am. Chem. Soc.*, 2003, **125**, 4119–4124.
31 W. Tantawy and H. Zipse, *Eur. J. Org. Chem.*, 2007, 5817–5820.
32 (*a*) S.-H. Ueng, M. M. Brahmi, E. Derat, L. Fensterbank, E. Lacôte, M. Malacria and D. P. Curran, *J. Am. Chem. Soc.*, 2008, **130**, 10082–10083; (*b*) S.-H. Ueng, A. Solovyev, X. Yuan, S. J. Geib, L. Fensterbank, E. Lacôte, M. Malacria, M. Newcomb, J. C. Walton and D. P. Curran, *J. Am. Chem. Soc.*, 2009, **131**, 11256–11262.
33 J. Jin and M. Newcomb, *J. Org. Chem.*, 2008, **73**, 4740–4742.
34 Y. Feng, L. Liu, J.-T. Wang, H. Huang and Q.-X. Guo, *J. Chem. Inf. Comput. Sci.*, 2003, **43**, 2005–2013.
35 Z. I. Watts and C. J. Easton, *J. Am. Chem. Soc.*, 2009, **131**, 11323–11325.
36 For reviews see: (*a*) P. Nordlund and P. Reichard, *Annu. Rev. Biochem.*, 2006, **75**, 681–706; (*b*) M. Bennati, F. Lendzian, M. Schmittel and H. Zipse, *Biol. Chem.*, 2005, **386**, 1007–1022; (*c*) M. Kolberg, K. R. Strand, P. Graff and K. K. Andersson, *Biochim. Biophys. Acta, Prot. Prot.*, 2004, **1699**, 1–34; (*d*) J. Stubbe, D. G. Nocera, C. S. Yee and M. C. Y. Chang, *Chem. Rev.*, 2003, **103**, 2167–2201; (*e*) H. Eklund, U. Uhlin, M. Färnegardh, D. T. Logan and P. Nordlund, *Prog. Biophys. Mol. Biol.*, 2001, **77**, 177–268; (*f*) J. Stubbe and W. A. van der Donk, *Chem. Rev.*, 1998, **98**, 705–762.
37 H. Zipse, E. Artin, S. Wnuk, G. J. S. Lohman, D. Martino, R. G. Griffin, S. Kacprzak, M. Kaupp, B. Hoffman, M. Bennati, J. Stubbe and N. Lees, *J. Am. Chem. Soc.*, 2009, **131**, 200–211.
38 J. Fritscher, E. Artin, S. Wnuck, G. Bar, J. Robblee, S. Kacprzak, M. Kaupp, R. G. Griffin, M. Bennati and J. Stubbe, *J. Am. Chem. Soc.*, 2005, **127**, 7729–7738.
39 P. E. M. Siegbahn, *J. Am. Chem. Soc.*, 1998, **120**, 8417–8429.
40 M. Mohr and H. Zipse, *Chem.–Eur. J.*, 1999, **5**, 3046–3054.
41 H. Zipse, *Org. Biomol. Chem.*, 2003, **1**, 692–699.
42 V. Pelmenschikov, K.-B. Cho and P. E. M. Siegbahn, *J. Comput. Chem.*, 2004, **25**, 311–321.